A new analytical model for the surface electric field distribution and breakdown voltage of the SOI trench LDMOS*

Hu Xia-Rong(胡夏融)†, Zhang Bo(张 波), Luo Xiao-Rong(罗小蓉), Wang Yuan-Gang(王元刚), Lei Tian-Fei(雷天飞), and Li Zhao-Ji(李肇基)

State Key Laboratory of Electronic Thin Films and Integrated Devices, University of Electronic Science and Technology of China, Chengdu 610054, China

(Received 1 December 2011; revised manuscript received 27 December 2011)

A new analytical model for the surface electric field distribution and breakdown voltage of the silicon on insulator (SOI) trench lateral double-diffused metal-oxide-semiconductor (LDMOS) is presented. Based on the two-dimensional Laplace solution and Poisson solution, the model considers the influence of structure parameters such as the doping concentration of the drift region, and the depth and width of the trench on the surface electric field. Further, a simple analytical expression of the breakdown voltage is obtained, which offers an effective way to gain an optimal high voltage. All the analytical results are in good agreement with the simulation results.

Keywords: silicon on insulator (SOI), trench, lateral double-diffused metal-oxide-semiconductor (LDMOS), breakdown voltage

PACS: 85.30.De, 85.30.Tv **DOI:** 10.1088/1674-1056/21/7/078502

1. Introduction

Lateral double-diffused metal-oxide-semiconductor (LDMOS) transistors have been widely used as integrated high-voltage switches and drivers in mixed-signal integrated circuits. An oxide trench is incorporated into the drift region. Firstly, the oxide trench can increase the electric-field strength along the x direction, which is similar to enhanced dielectric layer field technology.[1−6] Secondly, the drift region is folded in the y direction, resulting in multiple-directional depletion. These findings result in an enhanced breakdown voltage (BV) as well as a shortened drift length and cell pitch. Much research shows that high breakdown voltage is maintained, while the specific on-resistance (R_{on}) is reduced,[7−14] but all of these studies are based on numerical results. So far, there has been no analytical model for the silicon on insulator (SOI) trench LDMOS.

The purpose of this paper is mainly to develop a two-dimensional (2D) analytical model of the surface electric field and potential distribution, based on the Laplace solution and Poisson solution, to explore the physical mechanism of the SOI trench LDMOS. The dependence of the surface electric field on the depth and width of the oxide trench is discussed in detail, which indicates the validity of the model. Useful design curves of the breakdown voltage are obtained, indicating the dependence of the breakdown voltage on the width of the trench and the maximum electric field in the trench area. Numerical simulations are shown to support the analytical model.

2. Analytical model

The cross section of the SOI trench LDMOS is shown in Fig. 1, where W_T (D_T) is the width (depth) of the oxide trench, which is placed between the source and drain. t_S and N_D are the thickness and doping concentration of the SOI layer, respectively, t_{ox} is the thickness of the buried oxide layer (BOX), ε_{ox} is the relative dielectric constant of the BOX and the oxide trench, while ε_s is the relative dielectric constant of the drift region. The x and y directions are plotted in Fig. 1. When the device is biased in the off-state and the drift region is fully depleted, the potential function $\varphi_1(x, y)$ of the trench area must satisfy the 2D Laplace equation and the potential function $\varphi_2(x, y)$

*Project supported by the National Natural Science Foundation of China (Grant Nos. 61176069 and 60976060) and the National Key Laboratory of Analogue Integrated Circuit, China (Grant No. 9140C090304110C0905).

†Corresponding author. E-mail: h1_x2_r3@126.com

© 2012 Chinese Physical Society and IOP Publishing Ltd

of the SOI layer must satisfy the 2D Poisson equation, i,e.,

$$\frac{\partial^2\varphi_1(x,y)}{\partial x^2}+\frac{\partial^2\varphi_1(x,y)}{\partial y^2}=0, \tag{1}$$

$$\frac{\partial^2\varphi_2(x,y)}{\partial x^2}+\frac{\partial^2\varphi_2(x,y)}{\partial y^2}=-\frac{qN_{\rm D}}{\varepsilon_{\rm s}}. \tag{2}$$

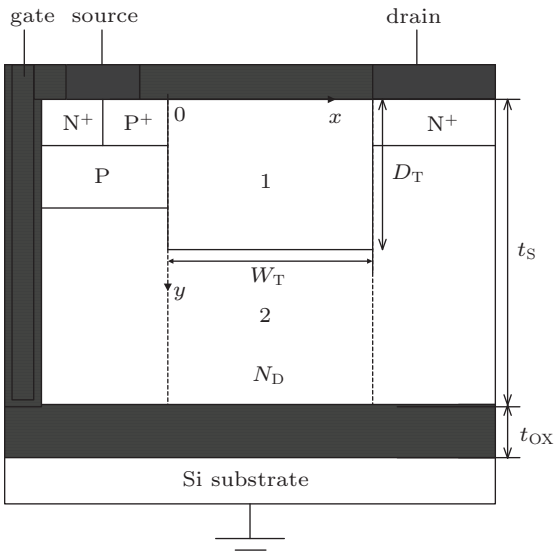


Fig. 1. Schematic drawing of the cross section of the SOI trench LDMOS.

The boundary conditions for $\varphi_i(x,y)$ $(i=1,\ 2)$ are given as

$$\left.\frac{\partial\varphi_1(x,y)}{\partial y}\right|_{y=0}=0, \tag{3}$$

$$\left.\frac{\partial\varphi_2(x,y)}{\partial y}\right|_{y=t_{\rm S}}=-\frac{\varepsilon_{\rm ox}}{\varepsilon_{\rm s}}\frac{\varphi_2(x,t_{\rm s})}{t_{\rm ox}}, \tag{4}$$

$$\varphi_2(x,D_{\rm T})=\varphi_1(x,D_{\rm T}), \tag{5}$$

$$\frac{\partial\varphi_2(x,D_{\rm T})}{\partial y}=\frac{\varepsilon_{\rm ox}}{\varepsilon_{\rm s}}\frac{\partial\varphi_1(x,D_{\rm T})}{\partial y}, \tag{6}$$

$$\varphi_1(0,0)=0,\quad \varphi_1(W_{\rm T},0)=V_{\rm d}. \tag{7}$$

In Eq. (3), it is assumed that the vertical electric field at the semiconductor surface may be minimized. Equation (4) is the continuity of the electric flux density across the Si/SiO_2 boundary. Equations (5) and (6) are the continuity equations of the potential and electric field along the boundary between 1 and 2, respectively. Equation (7) is the voltage condition imposed on the device.[15−18] The potential function $\varphi_i(x,y)$ can be approximated by the two-order Taylor expansion formula as follows:

$$\varphi_1(x,y)=\varphi_1(x,0)+\frac{\partial\varphi_1(x,0)}{\partial y}y+\frac{\partial^2\varphi_1(x,0)}{\partial y^2}\frac{y^2}{2}, \tag{8}$$

$$\varphi_2(x,y)=\varphi_2(x,D_{\rm T})+\frac{\partial\varphi_2(x,D_{\rm T})}{\partial y}(y-D_{\rm T})+\frac{\partial^2\varphi_2(x,D_{\rm T})}{\partial y^2}\frac{(y-D_{\rm T})^2}{2}. \tag{9}$$

Substituting Eqs. (8) and (9) into Eqs. (1) and (2) under boundary conditions (3)–(6), we obtain a general differential equation for the surface potential distribution function

$$\frac{\partial^2\varphi_1(x,0)}{\partial x^2}-\frac{\varphi_1(x,0)}{T^2}=\frac{-q\gamma N_{\rm D}}{\varepsilon_{\rm s}}, \tag{10}$$

with

$$T=\left[0.5(t_{\rm s}-D_{\rm T})^2+0.5D_{\rm T}^2+\frac{\varepsilon_{\rm s}}{\varepsilon_{\rm ox}}t_{\rm ox}(t_{\rm s}-D_{\rm T})+t_{\rm ox}D_{\rm T}+\frac{\varepsilon_{\rm ox}}{\varepsilon_{\rm s}}(t_{\rm s}-D_{\rm T})D_{\rm T}\right]^{1/2}, \tag{11}$$

$$\gamma=\frac{0.5(t_{\rm s}-D_{\rm T})^2+\varepsilon_{\rm s}t_{\rm ox}(t_{\rm s}-D_{\rm T})/\varepsilon_{\rm ox}}{T^2}, \tag{12}$$

where T is the characteristic length of the device, and γ denotes the trench factor. The surface potential $\varphi_1(x,0)$ and the electric field $E_1(x,0)$ can be obtained by solving Eq. (10) under the boundary conditions (7) as follows:

$$\varphi_1(x,0)=\frac{q\gamma N_{\rm D}T^2}{\varepsilon_{\rm s}}+\left[V_{\rm d}-\frac{q\gamma N_{\rm D}T^2}{\varepsilon_{\rm s}}\right]\frac{\sinh(x/T)}{\sinh(W_{\rm T}/T)}-\frac{q\gamma N_{\rm D}T^2}{\varepsilon_{\rm s}}\frac{\sinh[(W_{\rm T}-x)/T]}{\sinh(W_{\rm T}/T)},\quad 0\le x\le W_{\rm T}, \tag{13}$$

$$E_1(x,0)=\left[V_{\rm d}-\frac{q\gamma N_{\rm D}T^2}{\varepsilon_{\rm s}}\right]\frac{\cosh(x/T)}{T\sinh(W_{\rm T}/T)}+\frac{q\gamma N_{\rm D}T^2}{\varepsilon_{\rm s}}\frac{\cosh[(W_{\rm T}-x)/T]}{T\sinh(W_{\rm T}/T)},\quad 0\le x\le W_{\rm T}, \tag{14}$$

where $V_{\rm d}$ is the applied voltage. It is worth noting that when $D_{\rm T}=0$, $T=\sqrt{0.5t_{\rm s}^2+t_{\rm ox}t_{\rm s}\varepsilon_{\rm s}/\varepsilon_{\rm ox}}$ and $\gamma=1$. Equations (13) and (14) can be applied to single reduced-surface-field (RESURF) SOI LDMOS without any modification.

3. Results and discussion

In order to verify the proposed model, 2D device simulation is performed using the MEDICI simulation tool. Figure 2(a) shows the analytical and numerical results of the surface electric field distributions for SOI trench LDMOS and single RESURF SOI LDMOS with the same cell pitch. A fair accordance between the analytical and numerical results may generally be found. The surface electric field of the SOI trench LDMOS is enhanced compared with that of the single RESURF LDMOS due to the lower permittivity of the oxide trench than that of the Si region. The

average surface electric field increases from 3.5×10^5 to 9.5×10^5 V/cm, resulting in a large increase in breakdown voltage. It can also be found in Fig. 2(a) that the breakdown voltage increases with $D_{\rm T}$ because the length of the folded drift region in the SOI layer increases. Figure 2(b) presents the numerical results of the relationship between the BV and drift region concentration under different values of $D_{\rm T}$. Optimal drift doping increases as $D_{\rm T}$ increases, resulting in an increase in the critical electric field in the Si region. Thus, the maximal electric field in the trench area increases, resulting in an improved BV.

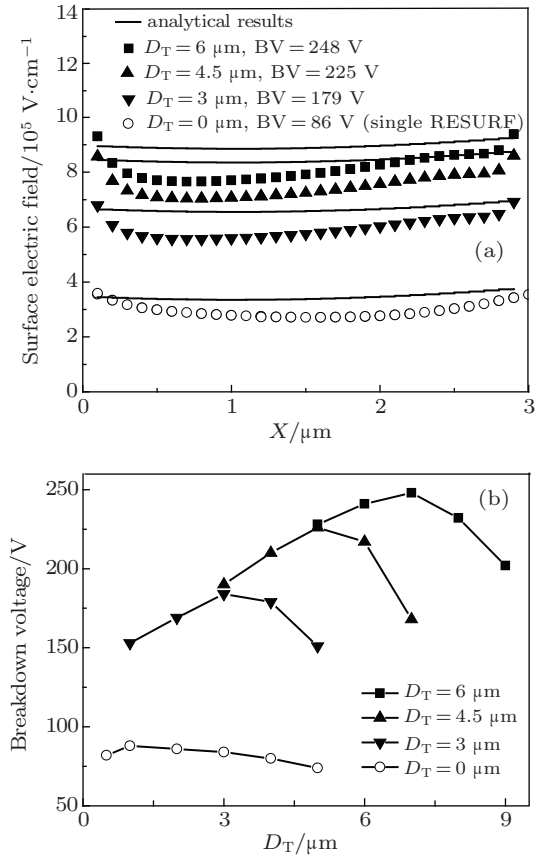


Fig. 2. (a) The analytical and numerical results of the surface electric field distribution of the SOI trench LDMOS and the single RESURF SOI LDMOS with the same cell pitch for different values of $D_{\rm T}$ and BV. (b) The dependences of simulated BV on optimal drift doping $N_{\rm D}$ for different values of $D_{\rm T}$. ($t_{\rm s}$ = 7.5 μm, $t_{\rm ox}$ = 1.5 μm, $W_{\rm T}$ = 3 μm.)

Figure 3(a) shows the influence of $W_{\rm T}$ on the surface electric field distribution. The analytical results are also in agreement with the numerical results. The maximal BV increases with $W_{\rm T}$ because both the length of the drift region and the oxide trench increase. The average surface electric field nevertheless decreases with $W_{\rm T}$, as seen in Fig. 3(a), and the optimal drift doping decreases as seen in Fig. 3(b), resulting in the decrease in the critical electric field in the Si region. Therefore, the maximal electric field in the oxide region decreases.

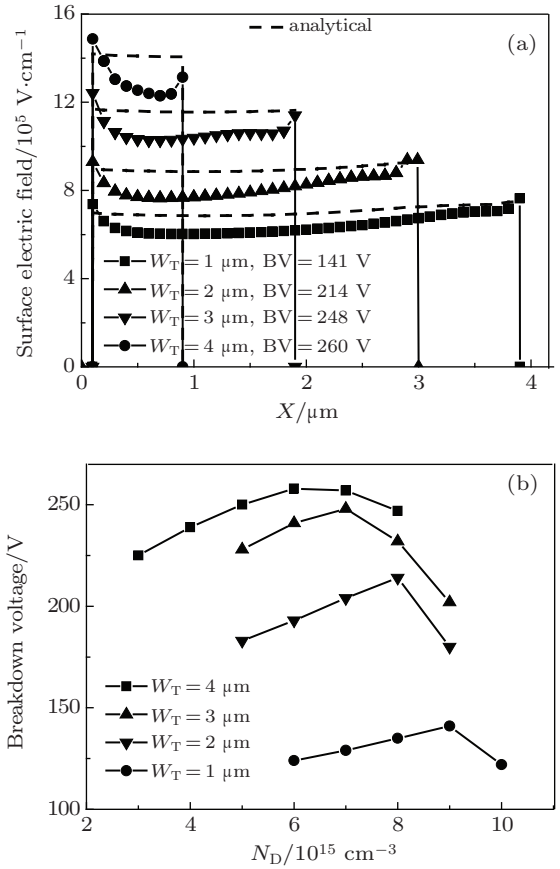


Fig. 3. (a) The analytical and numerical results of the surface electric field distribution of the SOI trench LDMOS for different values of $W_{\rm T}$. (b) The dependences of the BV on the optimal drift doping N_D for different values of $W_{\rm T}$. ($t_{\rm s}$ = 7.5 μm, $t_{\rm ox}$ = 1.5 μm, $D_{\rm T}$ = 6 μm.)

It can be seen in Figs. 2(a) and 3(a) that both the analytical and numerical results indicate that the surface electric field in the oxide trench is a rectangular distribution. This can be illustrated by the following expressions. Assume that the maximal electric field in the oxide trench is $E_{\rm Imax}$, then the optimal surface electric field distribution will be obtained when $E_1(0,0) = E_1(W_{\rm T},0) = E_{\rm Imax}$. In most cases, $D_{\rm T} > W_{\rm T}$, $\tanh(0.5W_{\rm T}/T) \approx 0.5W_{\rm T}/T$, then

$$\frac{2\gamma T^2}{W_{\rm T}} N_{\rm D} = \frac{E_{\rm Imax}\varepsilon_{\rm s}}{q}, \tag{15}$$

and the breakdown voltage is

$$\mathrm{BV} = 2qN_{\rm D}\gamma T^2/\varepsilon_{\rm s}. \tag{16}$$

Substituting Eq. (15) into Eq. (16), then the breakdown voltage of the SOI trench LDMOS is expressed as

$$\mathrm{BV} = E_{\rm Imax} W_{\rm T}. \tag{17}$$

Equation (17) indicates that the surface electric field can be considered as a rectangular distribution, which accords well with the simulation results. It also indicates clearly that if the $E_{\rm Imax}$ in the oxide region increases, then the cell-pitch can decrease while maintaining the same BV. To obtain the minimal cell-pitch, the $E_{\rm Imax}$ will be as high as possible. The $E_{\rm Imax}$ in the oxide trench area can be expressed as $E_{\rm Imax} = \varepsilon_{\rm s}E_{\rm s}/\varepsilon_{\rm ox}$ according to Gaussian law if the interface charge between the Si drift region and the oxide trench is neglected, where $E_{\rm s}$ is the critical electric field in the Si drift region. Thus, the maximal BV of the SOI trench LDMOS is BV $= \varepsilon_{\rm s}E_{\rm s}W_{\rm T}/\varepsilon_{\rm ox}$. Figure 4 shows the breakdown voltage and specific on-resistance as a function of the trench depth. Both BV and $R_{\rm on}$ increase with the increase in $D_{\rm T}$ because the length of the drift region increases. But no matter how deep the trench is, the BV is always lower than 315 V, which is the maximal theoretical breakdown voltage. The maximal simulation BV is 311 V, which is very close to the maximal analytical BV. This verifies the validity of the model. Figure 4 also reveals the optimal $D_{\rm T}$ value $D_{\rm T,op}$ for the 300 V SOI trench LDMOS. $D_{\rm T}$ is chosen as $D_{\rm T,op}$ when minimal $R_{\rm on}$ is obtained and the BV stops increasing.

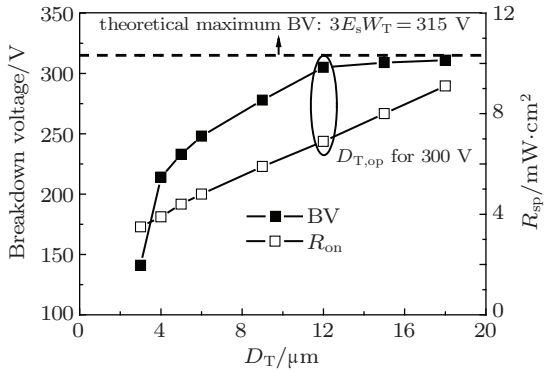


Fig. 4. Breakdown voltage and specific on-resistance $R_{\rm sp}$ as a function of trench depth. $t_{\rm ox} = 1.5$ μm, $W_{\rm T} = 3$ μm, $E_{\rm s} = 3.5 \times 10^5$ V/cm.

4. Conclusion

A new analytical model for the surface electric field distribution and breakdown voltage of the SOI trench LDMOS is presented in this paper. The model mainly accounts for the influence of the depth and width of the oxide trench on the surface electric field. Useful design curves of the breakdown voltage are obtained, indicating the dependence of breakdown voltage on the width of the trench and the maximal electric field in the trench area. All the analytical results are in agreement with the simulation results.

References

[1] Nakagawa A, Yasuhara N and Baba Y 1991 *IEEE Trans. Electron. Dev.* **38** 1650

[2] Wang Y G, Luo X R, Ge R, Wu L J, Chen X, Yao G L, Lei T F, Wang Q, Fan J and Hu X R 2011 *Chin. Phys.* B **20** 077304

[3] Wu L J, Hu S D, Zhang B and Li Z J 2011 *Chin. Phys.* B **20** 027101

[4] Luo X R, Zhang B and Li Z J 2007 *Solid-State Electron.* **51** 493

[5] Hu X R, Zhang B, Luo X R and Li Z J 2012 *Solid-State Electron.* **69** 89

[6] Zhang B, Li Z J, Hu S D and Luo X R 2009 *IEEE Trans. Electron. Dev.* **56** 2327

[7] Fujishima N, Sugi A, Andre C and Salama T 2002 *IEEE Trans. Electron. Dev.* **49** 1462

[8] Sona W S, Sohnb Y H and Choia S J 2004 *Microelectron. J.* **35** 393

[9] Varadarajan K R, Chow T P and Wang J 2007 *Proc. IEEE ISPSD* **233** 233

[10] Luo X R, Fan J, Wang Y G, Lei T F, Qiao M, Zhang B and Udrea F 2011 *IEEE Electron. Dev. Lett.* **32** 185

[11] Luo X R, Yao G L, Chen X, Wang Q, Ge R and Rlorin U 2011 *Chin. Phys.* B **20** 028501

[12] Zitouni M, Morancho F, Rossel P, Tranduc H, Buxo J and Pages I 1999 *Proc. IEEE ISPSD* **73** 73

[13] Theolier L, Mahfoz-Kotb H, Isoird K, Morancho F, Assie-Souleille S, and Mauran N 2009 *IEEE Electron. Dev. Lett.* **30** 687

[14] Mahfoz-Kotb H, Theolier L, Morancho F, Isoird K, Dubreuil P, Do Conto T 2008 *IEEE ISPSD* **303** 303

[15] Krizj D, Charitat G and Amon S 1996 *Solid-State Electron.* **39** 1353

[16] Chung S K 2000 *IEEE Trans. Electron. Dev.* **47** 1006

[17] Hua T T, Guo Y F and Gene S 2010 *IEEE ICSICT* 1850 1850

[18] Guo Y F, Li Z J and Zhang B 2006 *Microelectron. J.* **37** 861